Investigation of Low Temperature Cracking in Asphalt Pavements National Pooled Fund Study – Phase II

Task 1 – Literature Review

Mihai Marasteanu
Augusto Cannone Falchetto
Ki Hoon Moon
University of Minnesota

December 2009

TABLE OF CONTENTS

LIST OF FIGURES

Introduction

This literature review summarizes the research done in the area of low temperature cracking in the last three years (2006-2009). The purpose was to identify new developments in terms of test procedures, material selection, and data analysis that can be used in the follow up research effort part of Phase II. For each review, the main ideas of the research performed are briefly described and the benefits of the new reference to the current project and what was learned from it are presented. To better match the review with the various tasks of the current project, the summaries were divided into different sections.

Experimental Methods and Analyses

In this section, research efforts focused on laboratory experimental methods for both asphalt binders and mixtures are presented. Presently, thermal cracking specifications are based on strength and creep tests performed on asphalt binders and asphalt mixtures. For asphalt binders the Bending Beam Rheometer test (1) and the Direct Tension test (2) are used to determine the performance grade (3) based on tests performed on PAV binders (4). For asphalt mixtures, the Indirect Tension Tester (IDT) is used to perform creep and strength tests on cylindrical specimens loaded in compression along the diameter (5). A critical cracking temperature can be obtained at the intersection of the tensile strength-temperature master curve and the thermal stress-temperature master curve. This approach is also used in the TCMODEL subroutine of the new Mechanistic Empirical Pavement Design Guide (MEPDG)(6).

Binder and Mastic Testing

In the US, the PG system has been used for more than a decade to select and characterize asphalt binders. In Europe, only recently certain tests were adopted to specify asphalt binders or bitumens. For example Hase and Oelkers (7) used the BBR to investigate the influence of polymer type on low temperature properties. Twelve binders were tested according to DIN EN 14771 (8) at three different temperatures: –10°C, –16°C and –25°C. The results indicated, as expected, that the type of modification can influence both the stiffness and the relaxation properties of binders at low temperature, and that using the BBR can provide useful information for selecting an appropriate polymer modifier.

Khedoe et al. (9) conducted an investigation in which a stiff binder (C-fix) with a penetration of 9 at 25°C was compared to a conventional 70/100 pen grade bitumen. Direct Tension (DTT), which is not part of the European specifications, was used to perform tests on the two binders as well as mastic samples prepared with these binders. Tensile strength and strain at failure, as well as relaxation properties of the different materials, were determined. The results indicated that C-fix binder and mastics relaxed significantly less than the 70/100 binder and mastic. Additional experiments indicated that increasing the quantity of filler in the binder made the mastic stiffer and less relaxing; however, it increased stiffness and toughness. Two useful conclusions were drawn from this research: it is possible to use DTT to investigate the relaxation properties of asphalt binders and mastics; the addition of filler has both negative (less relaxation) and positive (increased strength and toughness) effects on binder low temperature properties.

In Canada, Yee et.al (10) developed an extended Bending Beam Rheometer test (BBR) protocol to take into account the effect of storage time on low temperature properties based on the "reversible aging" theory first introduced by Struik (11) and later applied to binders by Bahia (12) during SHRP research effort . Based on extensive experimental work, it was found that the double logarithmic shift rate μ, given by equation 1, is constant for a vast range of conditioning and loading times, with only minor deviations at short loading times and high stiffness.

$$\mu = \frac{-d(\log a)}{d(\log t_e)}$$ [1]

where:

a = shift factor used to overlap creep compliance curves,

t_e = time for the sample is equilibrated at cold temperature

This finding can be used to reasonably predict the creep stiffness and *m*-value without performing time consuming experiments. Although pavements cool over periods of weeks, obtaining long-term creep data as part of a binder grading protocol is not practical. For each binder, eight BBR beams were prepared, and were divided between two conditioning baths, which were set at −24°C (T+10) and −14°C (T+20). The samples were labeled *A1, A2, B1, B2, C1, C2, D1, and D2*. After 1 hour of conditioning at −24°C, samples A were tested at −24°C and Samples B were tested at −14°C. Samples B were conditioned at −14°C for 10 minutes before the data were collected. The average creep stiffness and m-values obtained after 60 seconds of loading were used to determine continuous grade temperatures at which S = 300 MPa or m = 0.3, for a conditioning time of 1 hour at −24°C. The same procedure was repeated for Samples C and D after 1 hour of conditioning at −14°C, but now Samples D were conditioned for 10 minutes before testing at −24°C. Immediately after testing, all samples were returned to their respective storage baths to be tested again after 1, 3, and 7 days of conditioning. (The 7-day conditioning period is not required in the MTO LS-308 test method but was considered useful in this particular investigation). From this study it can be concluded that the extended BBR protocol can be used effectively to identify better performing binders. In some instances, this approach may lead to a more economical solution than lowering the grade requirement, which requires more expensive polymer modified binders.

Due to its simplicity and repeatability, it is not surprising that the BBR procedure was targeted as a candidate test for specifying other types of asphalt based materials. A prime example is the work performed by Al-Qadi et al. (13), who developed a modified BBR test called Crack Sealant Bending Beam Rheometer test (CSBBR) to investigate the behavior of crack sealant at low temperature. Based on previous work performed by Zanzotto (14) and Zofka et al. (15), the authors proposed a modification of the machine and of the specimen size (thickness was doubled to reduce mid span deflection due to the soft characteristic of sealants). Good repeatability was obtained by preparing a homogenized sample. In their study, the authors used nine sealants (BB the softest, QQ the stiffest) that were expected to perform in a temperature range from -4 to -40°C. The sealant was also placed into a vacuum-pressure oven for 16 hours at 115°C to age. For the CSBBR a load of 980±10mN was applied for 240 seconds, followed by a seating load of 35±10mN for 480 seconds. To identify nonlinear effects, additional creep test were performed using 250, 490 and 980mN load levels. The results showed that the stiffness was independent of the applied stress level and that nonlinear effects were not present, see Figure 1. Further verification of the validity of the superposition principle in loading and unloading cycles was obtained using FEM simulations.
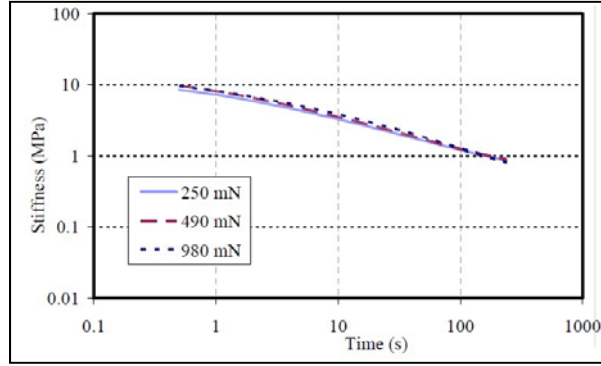
Figure 1: Creep stiffness measurement for sealant NN (13)

The authors also investigated the ability of the sealants to dissipate energy and maintain flexibility for a longer period time. The measured stiffness at 240 seconds was used to estimate stiffness after 5 hours of loading (5 hours is considered to be a proper time to dissipate the internal stresses due to relaxation phenomena) using the time temperature superposition principle. Three different temperatures were used to test stiff sealants (-40, -34, -28°C) and three for the soft ones (-16, -10, -4°C). The calculations indicated that after 5 hours, the materials "relaxed" 70-80% of the stiffness measured at 240 seconds.

In the analysis, the authors used a two-term Prony series model for creep compliance:

$$D(t) = \frac{1}{E_0} + \frac{1}{E_1}(1 - e^{-(t/\tau_1)}) + \frac{1}{E_2}(1 - e^{-(t/\tau_2)})$$ [2]

where:

$D(t)$ = the tensile creep compliance at time t;

E_i = material constants

τ_i = retardation time.

The Prony series parameters were used to calculate the dissipated and stored energy for each sealant.

$$W_{stored} = \sigma_0^2 \left[\frac{1}{2E_0} + \frac{1}{2E_1}(1 - 2e^{-(t/\tau_1)} + e^{-(2t/\tau_1)}) + \frac{1}{2E_2}(1 - 2e^{-(t/\tau_2)} + e^{-(2t/\tau_2)}) \right]$$

$$W_{dissipated} = \sigma_0^2 \left[\frac{1}{2E_1}(1 - e^{-(2t/\tau_1)}) + \frac{1}{2E_2}(1 - e^{-(2t/\tau_2)}) \right]$$ [3]

where:

W = is energy per volume

t = maximum loading time (240s)

σ_0 = stress in the outer fiber in the mid span.

and the energy dissipation ratio is calculated by the following expression:

$$ER = W_{dissipated} / W_{stored}$$ [4]

In this study, the aging effect on sealant was also investigated. The results showed that aged sealant became stiffer, and the stiffness increment depends on the chemical compositions.

Moreover in checking constitutive modeling of crack sealant behavior, the model developed by Elseifi (16) was used where the crack sealants behave as a viscoelastic material. The stiffness E(t) of a linearly viscoelastic material was expressed as a normalized Prony series as:

$$\frac{E(t)}{E_0} = 1 - \sum_{i=1}^{K} \varsigma_i (1 - e^{-t/\tau_i})$$

[5]

   where:

   E_0 = initial modulus

   ζ_i = normalized parameter defined as the ratio between relaxation strength and E_0

   τ_i = relaxation time.

In addition to the experimental investigation a finite element model was used to validate the sealant constitutive model. The deflection at the mid-span of the beam obtained from the FE model was compared to the experimental results showing that the Prony series satisfactorily simulates the results of bituminous crack sealant deformation for 240 seconds and 480 seconds of loading and unloading, respectively, at low temperatures.

Mixture Testing

Research performed at the University of Minnesota indicated that the Bending Beam Rheometer (BBR) could also be used to test thin asphalt mixture beams to obtain reliable measurements of creep compliance (15). However, small size specimens that contain a limited volume of material may not be representative of larger size specimens and real pavement conditions. Velásquez et al. (17) investigated this critical aspect by performing three point bending creep tests on beams of different sizes. A total of 10 laboratory mixtures were tested. Low temperature three point bending creep tests were performed on specimens with three different sizes: 6.25×12.5×100 mm (1x), 12.5×25×200 mm (2x), and 18.75×37.5×300 mm (3x) (Figure 2). The temperature effect on the representative volume element was studied by performing bending creep tests at three temperatures: high temperature (HT) level (PG low limit +22°C), intermediate temperature (IT) level (PG low limit + 10°C), and low temperature (LT) level (PG low limit −2°C).

Figure 2: 1x, 2x, and 3x asphalt mixture beam specimens. (17)

Statistical analyses were performed in order to evaluate the influence of various parameters like the size of the specimen, PG of the binder, aggregate type, loading time and temperature on the creep stiffness of asphalt mixtures. It was found that as the temperatures decreases, the mismatch between the stiffness of aggregates and of the binder (mastic) diminishes and the creep stiffness of asphalt mixture becomes less dependent on the size and distribution of aggregate particles. The effect of the beam size on the creep stiffness was negligible at intermediate temperature. At high temperature, the difference between the stiffness of the aggregates and the asphalt binder (mastic) started to increase and the mechanical response of the mixture became dependent on the

size of the aggregates. At the lowest test temperature, other factors, such as the difficulty of measuring very small deflection and the formation of layers of ice on the supports and around the extensometers, influenced the results and made the comparison difficult.

The current Indirect Tension Tester (IDT) (5) was used by Apeagyei et.al (18) to investigate the cracking resistance of antioxidant modified asphalt (AOX) mixtures; a common cause of increased asphalt stiffness is the oxidative hardening that occurs during asphalt mixture production and service life. Asphalt mixtures prepared with one AOX-modified asphalt binder, one un-modified asphalt binder, and typical limestone aggregates from Illinois quarries were prepared in the laboratory. Two levels of mixture aging at 135°C were considered: short-term oven aging (STOA) of loose mix in a forced-draft oven for two hours and long-term oven aging (LTOA) for eight hours. E* tests were performed at -10°C, 4°C, and 20°C using frequency sweeps of 0.01 Hz, 0.1 Hz, 0.5 Hz, 1 Hz, 5 Hz, 10 Hz, and 25Hz in the indirect tension mode using procedures recommended by Kim et al.(19). Standard AASHTO creep compliance tests were performed at temperatures of -20°C, -10°C and 0°C, and indirect tensile strength tests were performed after creep testing -10°C using the standard loading rate of 12.5 mm/min. Two models, Voight-Kelvin and a power-law model were fit to the creep compliance data to obtain the master curve for each mixture. Creep compliance decreased with increasing levels of aging and this effect was less pronounced in the antioxidant modified mixtures. It could be seen that aging resulted in a slight increase in tensile strength for both the modified and unmodified mixtures. The average tensile strength was higher in the modified mixtures in comparison with the unmodified. The study concluded that there is benefit to using antioxidant modifiers with respect to low temperature properties.

Katicha and Flintsch (20) used IDT testing and analyses to show that a linear elastic approach is not adequate to account for possible differences between tensile and compressive HMA properties. The stress distribution in a bimodular IDT specimen was investigated based on the Ambartsumyan model, (21, 22) for different compressive to tensile modulus ratios. The distribution was obtained through an iterative procedure since, in the constitutive equations of the Ambartsumyan material, the stress-strain constitutive relationship is a function of the principal stresses values and directions. The analysis showed that: as the compressive to tensile modulus increases, the tensile stresses throughout the specimen decrease; as the compressive to tensile modulus increases, the compressive stresses near the vertical diameter (loading diameter) increase; as the compressive to tensile modulus increases the compressive stresses away from the vertical diameter decrease.

Other authors (23) used IDT test data and Displacement Discontinuity Method (DDM) to predict asphalt mixtures fracture energy density in a Bending Beam Test. Voronoi tessellation theory and 2-D simulation method were also used. The experimental tests were performed at 10°C on nine Bending Beam test specimens (three replicates for each mixture) The strain value at failure were estimated at the point of first fracture and the fracture energy densities were computed as the resulting area under the stress-strain curve up to the fracture point. The simulation showed there is a considerable damage prior to reaching the peak of the stress-strain curves in all the tests and that prior to peak load the first fracture takes place. The results showed that DDM is able to characterize the fracture behavior of asphalt concrete at low temperature and provides acceptable predictions of fracture energy density.

Although the Thermal Stress Restraint Specimen Test (TSRST) is not part of the current AASHTO specifications, many researchers, in particular in Europe, have used it to study low

temperature cracking of asphalt pavements. Sauzéat et.al (24) analyzed thermo-mechanical effects, in particular the characterization of cracking and propagation of cracks at low temperature, based on results from TSRST and direct tension tests performed on mixture specimens instrumented with Acoustic Emission sensors. The loading system had a capacity of 50kN both in traction and compression, and allowed for a minimal speed of 6.4×10^{-6} mm/min. Three non-contact transducers located on two rings in the central part of the specimen were used to measure displacements. The initial distance between these rings was 9 cm for a 12 cm high specimen. The device for measuring the Acoustic Emission used three piezoelectric sensors with a contact surface of 15 mm diameter and a bandwidth range from 50 to 200 kHz. Using the measured wave parameters, the energy could be estimated in two ways: the envelop energy, computed from the area of the signal (mV. μs), and the true energy calculated from the integral of the square signal (10^{-18} J). The localization of the micro-cracks, which creates the acoustic emission, was performed by specific software. The TSRST was started at 5°C and at a cooling rate of 10°C/h. Some issues related to failure location prompted the authors to use specimen thinned in the central region. However, preparing such specimens may result in specimen damage before tests were conducted. Uniaxial tension tests (UTT) were also performed at different temperatures using a strain rate equal to 300×10^{-6}/h. From the TSRST test, it was shown that the thinned specimen yielded almost the same results as the cylindrical shape. The direct tension test showed that at low temperatures the mixtures tested were brittle, while at high temperatures they were ductile, with no clear transition phase. The stress-strain behavior was significantly affected by strain rate at high temperatures; at low temperature, the strain rate effect was not significant, suggesting that the behavior under very small strain rates, similar to those observed in pavements under low temperature, can be predicted from tests performed at higher strain rates.

Uniaxial tension test were also performed by Khedoe et al. (9). Three types of tests were performed on Porous Asphalt Concrete (PAC) gyratory compacted mixtures specimens: relaxation in displacement-controlled tests, relaxation in temperature controlled tests, and tensile strength tests. The research team concluded that adding filler to the C-fix binder material has both a stiffening effect as well as toughening effect, which matches the Direct Tension Test results on binders and mastics and that mastic behavior appears to be the driving force in terms of relaxation properties.

Hase and Oelkers (25) used uniaxial tension test, performed on prismatic asphalt mixture specimens, to investigate the influence of polymer modified bitumen (PmB) on life cycle analysis at low temperature. Stone mastic asphalt 0/8S (SMA) and binder course asphalt 0/16S (BCA) were evaluated at low temperatures based on uniaxial tension tests and cooling tests (Figure 3) using a standardized testing procedures(26). The parameters investigated from the uniaxial tension test were the maximum stress (tensile strength) $\beta_t(T)$ and the corresponding tensile failure strain $\varepsilon_{failure}(T)$ at the test temperature T. From the cooling test, the progression of the "cryogenic" stress over the temperature $\sigma_{cry}(T)$ and the failure stress $\sigma_{cry, failure}$ at the failure temperature $T_{failure}$ were obtained. Figure 3 shows the results of uniaxial tension tests in terms of tensile strength reserve. The tensile strength reserve was computed as the difference between the tensile strength and the cryogenic stress at the same temperature T:

$$\Delta \beta_t(T) = \beta_t(T) - \sigma_{cry}(t) \tag{6}$$

From further statistical analyses and taking into consideration traffic effects, it was shown that cryogenic tensile stress is an important factor in the predicted pavement life and cannot be disregarded.

It should be mentioned that the UTT test, similar to TSRST, is not widely used due to specimen alignment problems in direct tension tests in general. A small deviation from vertical alignment of the sample leads to uneven stress distribution in the specimen and to bending effect that can affect the reliability of the results.
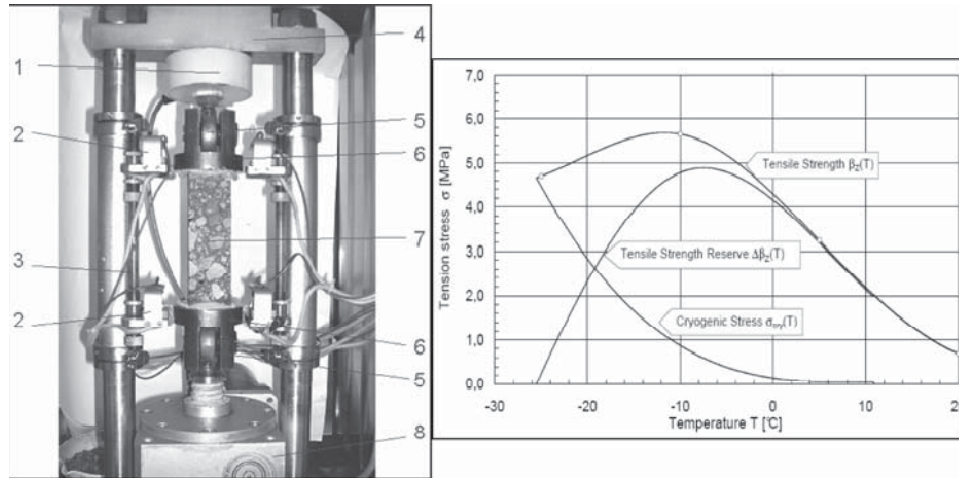
Figure 3: a) Uniaxial tension test device; b) Tensile strength reserve plot. (25)

Koh et al. (27) proposed an alternative type of test to determine the asphalt mixture properties. This test method, according to the authors, can reduce the disadvantages of IDT and UTT tests, and allows direct tension testing of gyratory compacted specimens or field cores of various types of mixtures (dense-graded, open-graded) of different thicknesses (thin or thick). The Dog-Bone Direct Tension test (DBDT) also has the advantage of having the failure plane known a priori, which allows measuring failure limits directly on the failure plane. Because of the specimen geometry, stress concentrations near the ends of specimen are less critical, and the location where failure is likely to occur is maximized. The DBDT specimens can be produced by simply coring opposing sides from slices or disks obtained from cylindrical laboratory samples or field cores. To optimize the specimen geometry, two-dimensional finite element analysis was conducted and, based on predicted stress distributions for two-inch wide specimens, a coring radius of 75.9 mm and a coring overlap of 50.8 mm were selected. The DBDT system is composed of several pieces, including a specimen coring jig, a dual cylinder tensile load equalizer, specimen loading heads, strain gage sensors and attachment kits, and a PC controlled servo-hydraulic load frame with an integrally mounted environmental chamber (Figure 4).

Figure 4: Dog-bone direct tension test prototype (27)

Finite element analysis was used to develop correction factors to accurately determine stress and strain based on simple equations from extensometers measurements obtained on the faces and edges of the DBDT specimens. The accuracy of the DBDT was verified with a Delrin specimen of known modulus. Tests on Open Graded Friction Course (OGFC) mixtures have shown promising results and the authors concluded that the effect of open graded friction course on top-down cracking performance may be evaluated based on tensile properties obtained from the DBDT procedure.

Fracture Test Methods

The test methods previously presented do not allow using fracture mechanics concepts since the test specimens are considered homogeneous with no crack present and therefore, no possibility to monitor crack propagation with loading. This type of analysis requires testing notched specimens and controlling the load based on crack growth to obtain post peak behavior related to crack propagation.

The Single Edge Notched Beam SE(B) Test (Figure 5) is the most documented method to determine fracture properties based on linear elastic fracture mechanics (LEFM) conditions(28).
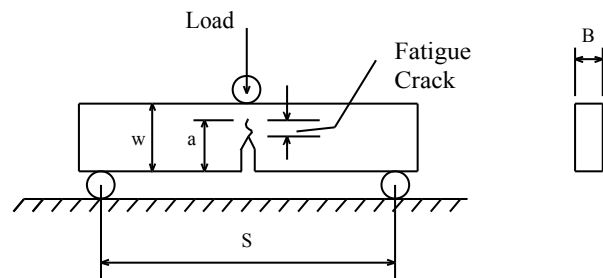
Figure 5: Single edge notched beam test (28)

Portillo and Cebon (29) used a three-point bending test for bitumen and idealized asphalt mix specimens to study the fracture behavior over a wide range of temperatures and loading rates, in order to develop a failure mechanism map to characterize the response of these materials similar to the failure mechanism pattern for bitumen films previously reported by Harvey and Cebon (30). The idealized mixture consisted of pure bitumen and 64% volume fraction of sub spherical sand particles between 150 and 300μm in size. The experimental data was used to calculate key

fracture parameters, such as stress intensity factor K_{IC}, fracture energy G_{IC}, and J-Integral J_{IC}. A 3-point bending fixture was designed to carry out fracture tests on pure bitumen and bituminous mixtures, see Figure 6.
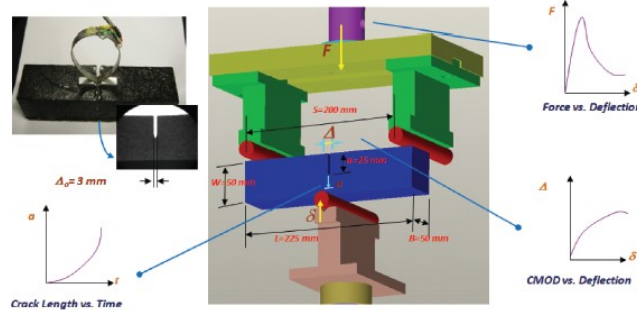
Figure 6: 3-Point bend experimental setup (29)

All tests were conducted under constant axial displacement rate control and a spring steel chip gauge was used to measure the crack mouth opening displacement. Crack length analysis was conducted using an optical system. The system comprised of an analog video camera located outside the environmental chamber which photographed the test specimen through a window. A flashing LED light signal was used to synchronize the time signals recorded on the video and the servo-hydraulic testing machine.

Fracture 3-point bending tests on pure bitumen specimens were conducted at temperatures ranging from −30°C to 0°C; the values of stress intensity factor K_{IC}, fracture energy G_{IC} showed to be similar to the results of Genin and Cebon (31) (Figure 7).

Author	Test		Test Temperature	K_{IC} (MPa m$^{1/2}$)	G_{IC} (J/m^2)
Portillo and Cebon	3Point Bend SE(B)		-20 ºC	0.01 - 0.04	2 – 13
			-30 ºC	0.06 – 0.1	5 - 11
Genin and Cebon (2000)	Plug Pull-Out		-20 ºC	0.02 - 0.05	
Harvey and Cebon (2005)	DCB		-30 ºC		5 - 10

Figure 7: Comparison table (29)

Temperature-compensated crack mouth opening strain rate $\dot{E}_T$ was defined to compare experimental results from tests at different temperatures and load rates as:

$$\dot{E}_T = \frac{\dot{\Delta}}{\Delta_0} \exp\left[\frac{-Q}{R}\left(\frac{1}{T_0} - \frac{1}{T_1}\right)\right] \qquad [7]$$

where:

Δ = the crack mouth opening displacement rate

Δ_0 = the initial notch width

Q = the thermal activation energy

R = the universal gas constant

T_0, T_1 = the reference temperature and test temperatures, respectively.

Similar results to the fracture mechanism map of Harvey and Cebon (32) were found: in the brittle region, the fracture energy is significantly lower than in the ductile region, indicating that the energy needed to initiate fracture is less at lower temperatures and high displacement rates. Idealized asphalt mixtures were tested on 3-point bending configuration over a temperature range from −30°C to 30°C. K_{IC} and fracture energy G_{IC} increased with an increase in temperature; this indicates that less potential fracture energy is needed for crack propagation at lower temperatures Failure mechanism maps showed ductile, brittle and transition failure regimes; moreover in the brittle regime when temperature decreased from −10°C to −30°C J-integral decreases showing that at lower temperatures resistance to crack growth is lower.

The beam geometry limits the use of SE(B) method on asphalt mixture gyratory specimens and field cores. An alternative geometry is used in the Disk Compact Tension DC(T) test, which was extensively investigated in the first phase of the current project.

The size effect on fracture property of asphalt concrete was investigated by Wagoner and Buttlar (31) using the Disk Shaped compact tension test DC(T), the size effect law (SEL) proposed by Bazant (34) and the boundary effect model. Testing was conducted with a single temperature of -10°C. Two sensitivity sets of test were performed: in the first four different diameters (100, 150, 300, 450 mm) with a constant 50 mm thickness were tested and in the second five thicknesses (from 25 to 150mm) and two diameters (150 and 300 mm) were selected. The crack mouth opening displacement was used as control parameter. CMOD was scaled accordingly to the specimen dimension.

Experimental and statistical results showed that diameter influenced the fracture energy and as it increases also the fracture energy increases. Also the specimen thickness affects the fracture energy especially in the range of 25-50 mm. As the thickness increased an increase in the fracture energy was experienced (Figure 8). It was concluded that fracture properties are affected by specimen size and this effect should be taken into account in modeling the pavement.
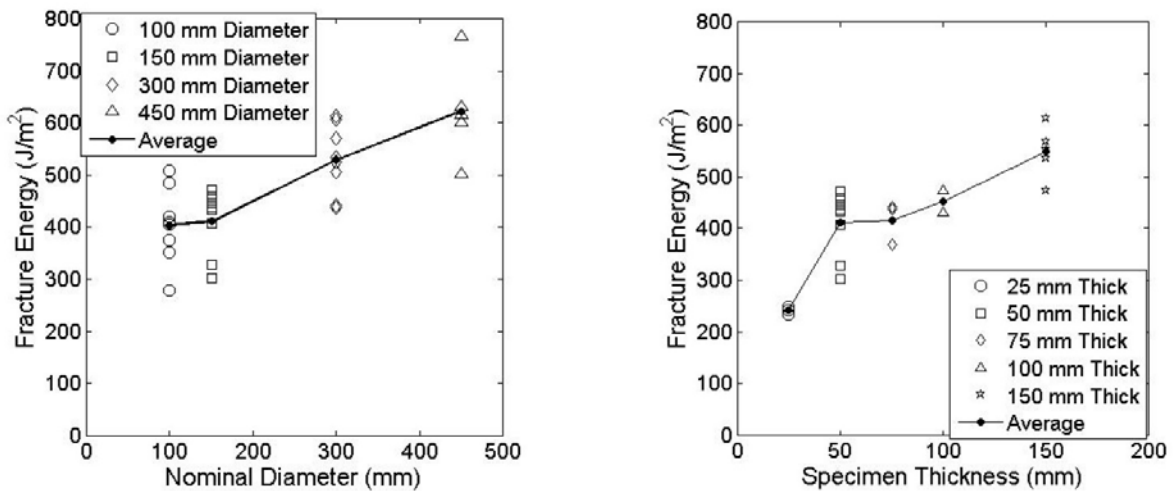
Figure 8: Variation of fracture energy with diameter and thickness (33)

In the size effect law analysis it was found that the selected size ranges were adequate to investigate the size effect. On the other hand the computed specific fracture energy, $G_f = 87.5J/m^2$ is only a portion of the total fracture energy; however it is able to capture the initial portion of the load displacement curve that is independent of the specimen size. The fracture process zone FPZ was estimated as 42.8mm and this value is in agreement with the 40mm length obtained in a previous study of Marasteanu et al. (35).

The size effect on fracturing of asphalt concrete based on DC(T) test was also investigated by Kim et al. (36) using Discrete Element Method (DEM). Cohesive softening model was employed to analyze asphalt fracture behaviors and DC(T) fracture tests were conducted for different sizes of asphalt concrete varying from 100 mm to 450 mm diameter. The different size specimens were modeled and simulated using homogeneous DEM fracture models with bulk viscoelastic properties. The experimental and numerical specimen size dependency of asphalt concrete was compared with the size effect law, which was proposed by Bazant (34). The size effect law may be expressed as:

$$\sigma_n = \frac{Bf_t}{\sqrt{1+\beta}} \hspace{3cm} [8]$$

where:

σ_n = nominal strength

f_t = tensile strength

β = brittleness number equal to d/d_0

d   = depth of the beam

$B.d_0$ = empirical constants.

It was found that the bulk viscoelastic DEM fracture model with the same material properties could predict the size effect on the nominal strength of asphalt concrete based on two sets of material properties. By comparing elastic and viscoelastic homogeneous DEM fracture models, it was shown that viscoelastic properties of asphalt concrete play an important role on the fracture behavior as the specimen size becomes larger. Heterogeneous fracture model for different specimen size was also implemented and applied for the investigation of size effects; however the calibration procedure of material parameters was necessary based on experimental test data. The global fracture responses obtained from the heterogeneous DEM models were matched well with experimental fracture behaviors in the force versus CMOD curves and a 3-D fracture analysis investigation was recommended.

In a previous study, Kim et.al (37) investigated the effects of material microstructure on fracture mechanics and the rate dependency of asphalt concrete using a cohesive zone model with bulk viscoelastic properties combined with bi-linear post-peak softening (Figure 9). Other aspects like material heterogeneity have been taken into account and a Discrete Element Method (DEM) model was implemented.
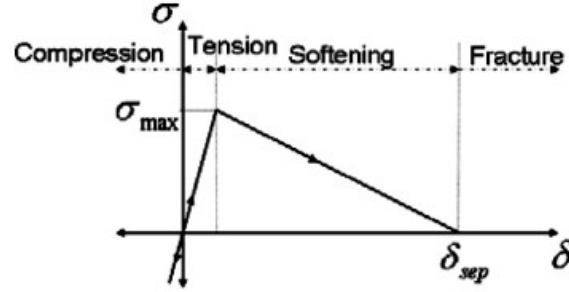
(c) Bilinear Cohesive Fracture Model

Figure 9: Bilinear Cohesive Fracture Model (37)

Two types of tests were performed on asphalt concrete mixture with PG 64-22. The fracture energy was obtained from DC(T) tests and viscoelastic properties were obtained from IDT tests. The creep compliance was measured at three temperatures (-20, -10 and 0°C). The indirect tension test was also used to measure the tensile strength at the intermediate temperature. The relaxation model parameters were used in the DEM fracture model. The elastic DEM fracture model simulation resulted in an over-prediction of the pre-peak load-CMOD behavior and under-predicts the global softening tail while viscoelastic DEM model was in better agreement with experimental results, even if the softening tail resulted in a slightly under-prediction. Different loading rates was also investigated in the case of the viscoelastic model showing that loading rate affects the softening tail and peak load as well as the initial slope of the global load-time curve. Overall the DEM fracture model seemed to be able to represent the rate-dependency of the asphalt mixture tested in the DCT: mixtures tested at higher loading rates showed more brittle behavior while post-peak softening behavior at lower loading rates was more evident. The shape of the predicted softening curve was improved including heterogeneity into the DEM model even though only the elastic simulation was performed. Microcracks, crack tortuosity, and bridging were better simulated by the heterogeneous microstructure underlining the importance of heterogeneity compared to the material viscoelasticity at the low temperatures.

Note that, in the case of the Boundary effect model, the energy consumed by the FPZ is considered as a material constant. Boundary limit can prevent the FPZ to fully develop. Hu and Wittmann (38) proposed a fracture process zone (FPZ) formed of an inner region W_{sf} and an outer region W_f (Figure 10).
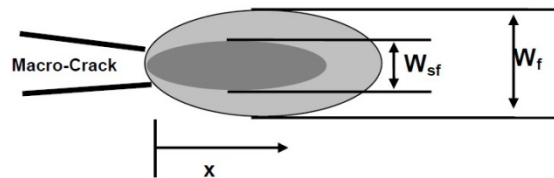
Figure 10: Fracture process zone according to Hu and Wittmann (38)

The size dependant fracture energy is then expressed as:

$$G_f = \frac{1}{W-a} \int_0^{W-a} g_f(x)dx \qquad\qquad [9]$$

Where:

W-a   = initial ligament length
g_f   = local fracture energy
G_f   = size dependant fracture energy

A bilinear assumption is adopted by the boundary effect model for the variation of the local fracture energy as the crack approaches the boundary of the specimen. The total fracture energy should increase until a critical specimen size is reached. Beyond that threshold the fracture energy becomes a constant since the FPZ is no more influenced by the specimen boundary. The results obtained by the authors showed that the model fit was acceptable and a size independent fracture energy of $G_F = 605$ J/m^2 with $a_l/W = 0.45$ was obtained.

Another simpler alternative to SE(B) is the Semi Circular Bend SCB test originally proposed by Chong and Kuruppu (39); this test was also investigated extensively in the first phase of the current project. Recently, Van Rooijen and de Bondt (40) used a draft procedure developed in the Netherlands, which was based on Paris' law, to study the crack propagation during cyclic SCB tests performed at relatively low temperature on one type of asphalt mixture prepared with five different binders. The proposed procedure is also based on Paris' law:

$$\frac{dc}{dN} = A \cdot K_I^n \qquad\qquad\qquad [10]$$

where:
c   = length of crack [mm]
K_I = stress intensity factor [MPa×mm$^{0.5}$]
N   = number of load cycles
A, n   = material parameters determined from the experimental results

The test method consists of four steps. In the first step, the maximum load F_{max}, the maximum load at failure $F_{failure}$, and the fracture strength K_{IC}, are predicted from a monotonic Semi-Circular Bending (SCB) test for each specimen. The crack opening displacement amplitude (COD) is then defined as the difference between maximum and minimum displacement during one load cycle. The crack length calculation is performed during the second step of the procedure based on finite element analysis. In the third part of this method the calculation of stress intensity factor, K_I, and stress level (σ_{SCB}) is carried out. Finally the material parameters A and n are determined.

Monotonic SCB test and cyclic SCB test were carried out on an asphalt binder/base course with a maximum nominal aggregate size of 11.2mm and 5.2% bitumen (of the total mixture) prepared with two types of standard penetration grade bitumen (i.e. Pen 40/60 and Pen 160/220) and three types of polymer modified binder (PMB). The load at failure obtained from the monotonic SCB test was used to determine the maximum load, F_{max}, for the cyclic SCB test. Tensile properties of the binders such as yield strain, strain at failure, and the deformation energy to failure, were determined with the force-ductility test (EN 13589 (41) and EN 13703(42)). After the test the following relationship between n and log(A) was obtained:

$$\log(A) = -1.4397 \cdot n - 2.5273 \qquad\qquad\qquad [11]$$

From the calculation of the stress intensity factor K_{IC}, the authors concluded that the duration of the crack propagation phase was relatively short for all binders, which is in disagreement with field experience that suggests that the effect of healing and creep should be taken into account.

An alternative tensile test, called Fenix, was developed by Perez et al. (43). The authors objective was to develop a procedure with a low cost set up to determine crack resistance through calculation of dissipated energy that would eliminate the difficulties associated with

SE(B) specimen preparation and SCB loading head compression testing issues. Fenix test is a traction test applied to a half cylindrical sample with a 6 mm depth notch, placed in the middle of the flat side of the specimen (Figure 11). The sample is fabricated with a gyratory-compactor and/or Marshall device. Two steel plates are fixed on the flat side separated by the notch. Steel plates are attached to the loading platen, allowing plates to rotate around fixed points once test has begun. Test is carried out under controlled displacement conditions. Displacement velocity is established at 1 mm/min. Temperature is chosen according to the environmental conditions that have to be reproduced.
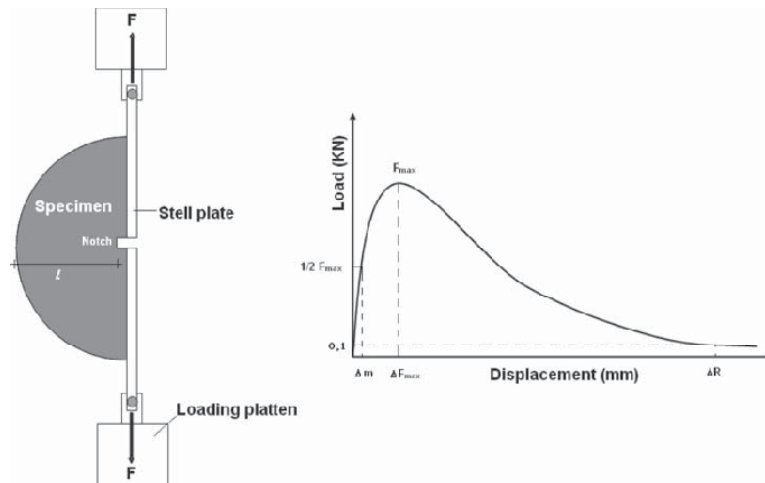
Figure 11: Fenix test and typical load vs. displacement output curve. (43)

The test calibration, obtained by sensitivity analysis, showed that Fenix test can be used over a wide range of test temperatures. It was found that it was possible to obtain and analyze mixture behavior in the post peak (softening) region.

Low Temperature Cracking Models

The experimental results and the analyses performed on the experimental results, obtained using the test methods previously described, provide the critical parameters required to develop models of the cracking phenomenon that can be incorporated in pavement performance prediction models.

Zbrowski and Kaloush (44) evaluated the capability of the TCMODEL in characterizing thermal cracking resistance of asphalt rubber mixture. Since this model doesn't properly estimate the asphalt rubber behavior, they developed a new method based on fracture energy parameter rather than on tensile strength at -10°C of the material and slope of creep compliance. Comparison of a traditional mixture and a gap graded asphalt rubber mixture showed that the latter mix behaves better than the traditional (Figure 12):
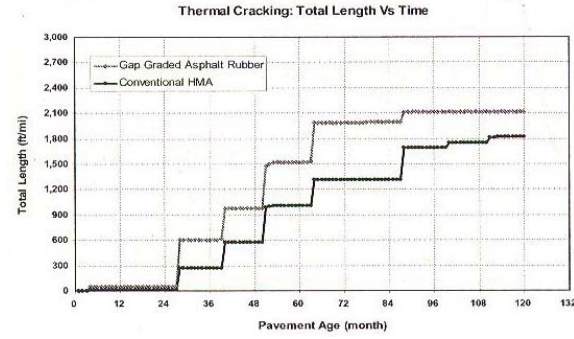
Figure 12: Thermal cracking prediction using MEPDG (44)

From fracture energy tests it was found that the asphalt rubber mixture had a two times higher fracture energy compared to a traditional mixture. A new method to calculate the crack propagation based on the total fracture energy, the creep compliance, D_1, in combination with the tensile strength maximum limit and the slope of creep compliance was developed based on the Superpave TCMODEL. The experimental part was based on eighteen conventional and twenty-one asphalt rubber mixtures. Based on the test results, thermal cracking prediction equations were obtained. The following modified creep compliance prediction equation was proposed:

$$\log(D_1^*) = 0.145 \cdot (-8.5246 + 0.0104T + 0.7956\log(V_a) + 2.0093\log(VFA) - 1.92231\log(A_{RTFO})) \quad [12]$$

where:
D_1^* (1/kPa) and m* are the fracture coefficients obtained from the creep compliance of the mixture;
T = Test temperature (°C)
V_a = Air Voids (%)
VFA = Void filled with asphalt (%)
Pen_{25} = Penetration (0.1 mm) at 25°C
A_{RTFO} = Intercept of binder Viscosity – Temperature relationship for the RTFO condition

An additional variable was included, the rubber percentage, to take into account the modification due to a crumb rubber and the following fracture energy expression was proposed:

$$\Gamma_{tfr} = 0.1129792 * (4497.832 - 439.057 * AC + 46.284 * AC^2 - 2057.821 * AV \quad [13]$$

$$+ 40.009 * AV^2 + 12612 * \log(V_{beff}) + 13571.050 * \log(VMA) - 345.948 * VFA$$

$$+ 8.056 * Pen_{25} - 0.052 * Pen_{25}^2 + 1.044 * AC * Rubber(\%)$$

where Γ_{tfr} is the fracture energy (Figure 13):

18
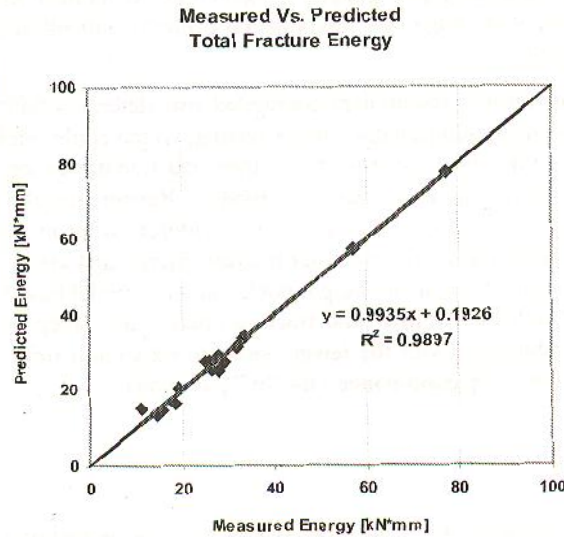
Figure 13: Measured versus predicted total fracture energy (44)

Based on previous research performed at University of Florida (45, 46), Kim et.al (45) developed an analytical model to evaluate the effect of thermal loading and mixture properties on cracking and dissipated creep strain energy (DCSE). TCMODEL and Prony series were used for the representation of the Creep compliance and irreversible creep strain. Knowing the thermal stress and the dissipated creep strain, the dissipated creep energy may be computed at each increment of time, Δt. On the other hand, $DCSE_f$ varies with temperature. Since DCSE is related to $DCSE_f$, the energy transfer can be obtained from a transformation of DCSE at a given temperature into DCSE at a reference temperature. Finally, the accumulated DCSE at any given time, t, is expressed by the following equation:

$$DCSE(t) = \sum DCSE(\Delta t)$$ [14]

The model used was represented by a thin plane with a central crack 10 mm length and a process zone of 5 mm. Four steps were implemented to compute the HMA thermal fracture: first the process zones are defined; second the thermal stresses are predicted; then the mean stresses in each process zone is calculated, and finally DCSE is evaluated. The following method is based on time increments and a 100 mm crack length was used as limit to stop the computation. The master curve and the energy transfer were obtained by setting the reference temperature as the lowest temperature (0°C).

A series of experimental tests, performed on a total of 99 specimens from eleven sections in Florida, were used to evaluate the model with a constant mixture thermal coefficient 2.0×10^{-5} 1/C. The model expresses the amount of cracks in function of time increments: a longer cracking time of mixture implies a good resistance to thermal damage.

Top-down cracking is not only related to the thermal cracking; the traffic load plays a fundamental role in the induced damage. The cracked and uncracked pavements were discriminated by the single failure time named Minimum Time Requirement (MTR) obtained from field data. This parameter was used to define the Modified Energy Ratio (MER) in such a way that it can take into account traffic load and thermal effects. The MER was expressed as:

19

Modify Energy Ratio (MER) = IFT/MTR [15]

Where:

IFT = Integrated Failure Time

MTR = Minimum Time Requirement

Good correlation between observed field performance and predicted top-down cracking was obtained.

Based on the IDT and E* results described in the previous section (see page 8), Apeagyei et al. (18) used TCMODEL to predict transverse cracking, expressed as length of cracks in meters per 500 meters of pavement. A theoretical pavement, approximately 300 mm (12 in.) thick, located in Minnesota, was simulated. It was determined that aging resulted in significant reduction in pavement life for all the mixtures. This analysis provided a useful quantitative measure of the benefit of antioxidant modified asphalt (AOX) in terms of thermal cracking pavement performance.

The authors also applied fracture energy concept and the method proposed by Zhang (48) to further investigate the effect of antioxidant modified asphalt (AOX) on cracking behavior. The Zhang method involves five steps in which Fracture Energy (FE) and Elastic Energy (EE) are first computed in order to obtain the Dissipated Creep strain energy threshold (DCSE$_f$) as the difference between FE and EE. The Dissipated Creep Strain Energy per cycle (DCSE/cycle) for load duration of 0.1 sec, the average stress σ_{AVE}, and maximum strain rate at 100 sec ε_{pmax} are then computed according to the following expressions:

$$\frac{DSCE}{cycle} = \int_{0}^{0.1} \sigma_{AVE} \sin(10\pi)\varepsilon_{p\max} \sin(10\pi)dt$$

$$\frac{DSCE}{cycle} = \frac{1}{20}\sigma_{AVE}^2 D_1 m(100)^{m-1}$$

[16]

Finally, creep compliance parameter, D_1, and the m-value are obtained during creep testing. Once the stress levels in the mixture and the DCSE/cycle are known the number of cycles required to reach the DCSE threshold at a given crack length are determined. The results showed that the number of cycles to DCSE$_f$ varies with stress level and that aging reduces the number of cycles (N) needed to reach DCSE$_f$. Comparison of the number of cycles for long term oven aging (LTOA) to short term oven aging (STOA) for a single stress level of 100 psi indicated that the use of antioxidants provided benefits against thermal cracking expressed by a decreased binder stiffness at lower temperatures and increased binder stiffness at high temperatures relative to the untreated control binder.

In a different research effort, the authors (49) investigated the effect of cooling rates on accumulation of thermal stresses in asphalt pavements. The experimental part was carried out on five mixtures from the SHRP General Pavement Study (GPS). Using a generalized Maxwell model the relaxation modulus master curves were obtained at a reference temperature of -20°C and thermal stresses were computed for different cooling rates (1, 2, 3, 5, 10°C/h). Thermal stresses were positively correlated with cooling rates up to 5°C/h; for higher values, the effect of cooling rate is less evident.

The cooling rate effects on asphalt pavement were also investigated using FEM simulations. The pavement structure of five MnROAD test cells were selected, and six cooling cycles, during which the pavement surface temperature drops from 0 to -30°C at different rates,

20

were simulated. As expected, stress accumulation was found dependent on cooling rate, and peak tensile stresses were found at -30°C.
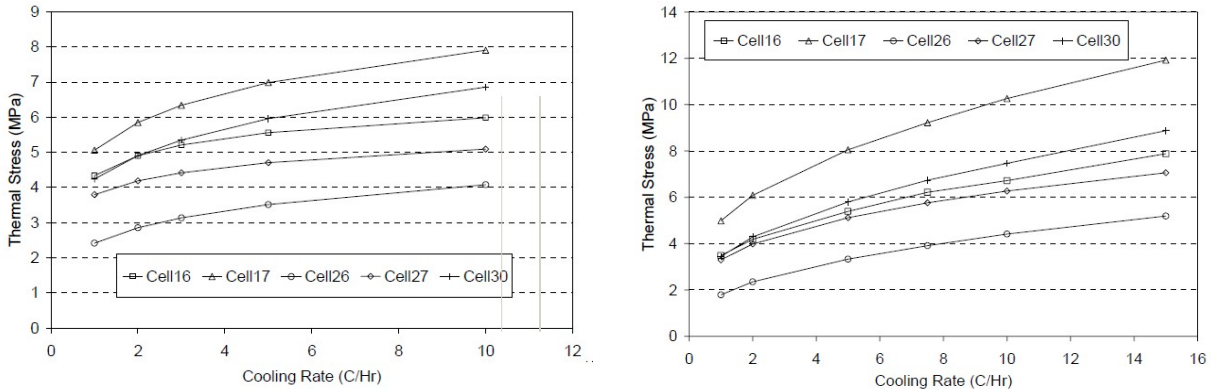
Figure 14: Comparison between analytical and FEM solution (at -30C) (49)

The TCMODEL was used to obtain pavement life predictions. A 45% reduction of service life was evaluated when the cooling rate increased from 2 to 3°C/h, and an additional average reduction of 32% was estimated for a cooling rate increase from 3 to 4°C/h. For the coolest single event, FE simulation and field data were in agreement, although the test sections were subjected to traffic loading and not only to thermal stresses. The model results were finally compared to AASHTO MEPDG performance predictions (50). Some differences were found between TCMODEL and FE and analytical solutions since the former is related to pavement serviceability level while FE and analytical solutions are related to the thermal stresses that develop at various cooling rates, but overall, the predictions compared well with the field performance.

Five MnROAD test cells, two from high volume traffic sections, and three from low traffic volume test loop) were used to perform an integrated laboratory study coupled with finite element simulation by Dave et.al (51). Creep compliance and the tensile stresses of each of the five specimens were obtained from Indirect Tension (IDT) while the fracture energy was measured using the Semi-Circular Bend (SC[B]), the Disk-Shaped Compact Tension (DC[T]), and the Single-Edge Notch Beam (SE[B]). Because of the different tests' configurations size effects and differences in fracture energy values were experienced. For this reason only the fracture energy obtained from the DCT was used in the numerical simulations. The FE simulation was performed in 5 steps. The FE models domain for low-temperature cracking simulations were constructed using graded meshes in order to reduce the computational requirements. Asphalt concrete was modeled using the generalized Maxwell model where model parameters were determined using the creep compliance data from laboratory testing. A cohesive zone model was adopted and the material parameters material strength (σ_t) and fracture energy (G_f) estimated through laboratory testing were input in the model. Thermal and traffic tire load was applied, moreover a critical condition approach in which the coolest pavement temperatures reached were identified was selected for the model simulation. In general, the simulation results were found to comply with field observations.

Traffic induced stresses and temperature-related stresses were addressed by Wistuba et al. (52) in correlation with the analysis of surface-initiated longitudinal cracking in asphalt pavements. Cracking resistance is investigated both with numerical analysis tools and laboratory

experimentation. The pavement was modeled as a multilayer system with an axle load acting on a circular area. The equation of energy balance and Fourier's linear heat condition law were used to obtain the pavement surface temperature and its variation in the pavement structure. The asphalt material was modeled with the power law model (linear spring and non-linear dashpot in series) while material parameters were obtained by uniaxial creep test and dynamic stiffness test. The numerical analysis provided evidence that the maximum horizontal tensile stresses are concentrated between the wheel paths and along the road axis and moreover allows seeing the separate effects of the temperature associated and traffic associated stresses. The experimental evaluation of cracking resistance was assessed by a Cyclic Tensile Stress Test (in order to simulate the traffic load). Furthermore thermal induced stress was simulated by applying a constant tensile stress to the asphalt specimen. Healing effects on the material was also addressed and then different loading conditions were selected from a real traffic spectrum and then separated in several groups. Each load groups was characterized by constant force amplitude, a specific number of load cycles and a uniform frequency. The rest period between two consecutive load pulse-groups was related to the time gaps between trucks. Based on traffic data rest periods of 3 seconds and 6 seconds were selected. The loading frequency was computed based on the time gaps between individual axles. Considering the different multiple axle configuration of HGVs, a time gap between the axles of 0.066 seconds was found and a 15Hz frequency was selected to perform laboratory testing for multiple axle configuration. For single axle configuration 5Hz frequency was adopted and four load modes were applied during testing. From the data obtained on the test it was evident that more load cycles are needed as test better approximate the real loading. Furthermore it was noted that stiffness modulus E* decreases with increasing number of load cycles in the case of fatigue. Relaxation effects were observed in the asphalt material during the rest time: thus a healing effect was experienced even at -15°C.

International Roughness Index (IRI) was used as a discriminating parameter in the investigation of thermal cracks on pavement by Bae et al. (53). An Automated Laser Profile System (ALPS) was used to measure the thermal cracks data form 14 cells from the mainline test roadway (at the MnROAD and for each cells three randomly selected crack were superimposed to a free crack pavement profile with different initial IRI (Figure 15).
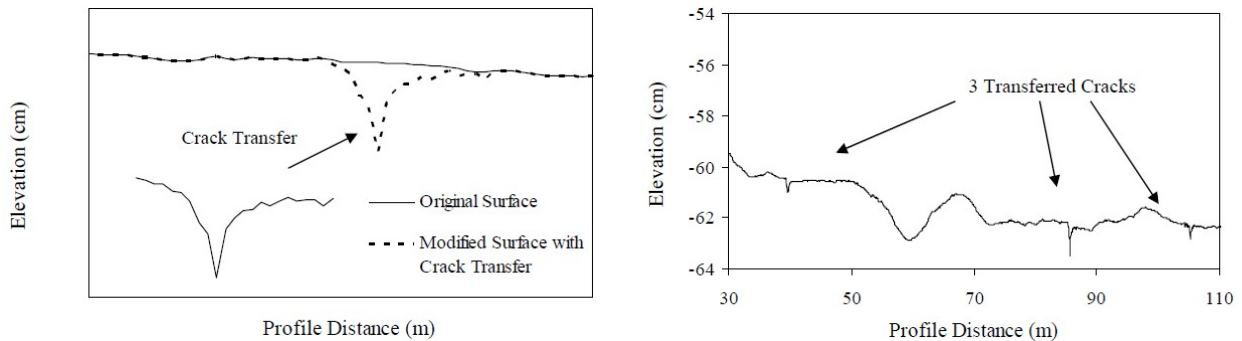
Figure 15: Crack-profile superposition (53)

From the computation of the final IRI it was found that the range of increment was of 0.06 to 0.2 m/km for a 1.20 m/km profile and of 0.01 to 0.1 m/km for the 4.33 m/km profile. Higher IRI profiles were found to be less sensitive to the cracks superposition compared to those with low IRI, but overall a significant IRI increment was experienced for all the profiles showing that cracks with amplitudes larger than 0.5 cm sensibly influence roughness. The IRIs for real pavement profiles with the actual number of cracks were also evaluated showing a considerable

increase in the IRI value. The annual increase in vehicle operating costs due to thermal cracks was estimated at 14,000 to 97,000$/km.

Other Relevant Studies

The Discrete Element Method (DEM), developed by Cundall and Strack (54) was used by Wu et.al (55) to simulate the monotonic compressive behavior of an idealized asphalt mixture in the elastic regime (low temperature, high strain rate). The effect of random variations in internal sample geometry, the distribution of bond strengths between adjacent particles and the coefficient of friction between particles were investigated with the use of the ITASCA software PFC-3D. A numerical sample containing 6,000 particles, 1.77mm in diameter was simulated with a particles density of 63.5% of the total volume and an average 5.8 contacts per particle. The post-peak (softening) behavior was modeled by allowing bond breakage when either normal or shear stress between contacting particles exceeds the normal or shear bond strength. Different friction coefficient, μ, ranging from 0 to 0.9 were evaluated showing that the compressive strength increases as the friction coefficient increases up to a value of 0.5 after which it remains approximately constant. In general it was found that 6,000 particles are required for reasonably accurate estimates of bulk material properties in the case of compressive strength. Moreover the random effect of particle position on predicted compressive strength is not significant in comparison to the variability in bond strength and the friction coefficient. The overall shape of the predicted stress-strain curve from the DEM approach showed a good agreement with the experimental results.

A micromechanics-based virtual testing procedure was presented and developed by Feng et al (56) to study the HMA cracking dependence on the interaction of the aggregate and asphalt binder. A lattice modeling methodology that incorporates a fracture energy based criterion is used to predict the mechanical behavior of HMA is coupled with a stand-alone virtual micro structure fabrication technique. A multi-scale modeling method that considers the effect of different aggregate sizes at different scales was used to reduce the computational cost while capturing the mechanical phenomena at various scale length. The method was validated comparing the simulation results of uniaxial tension test to those obtained from the physical tests (Figure 16). An aggregate gradation four-scale approach method (1 corresponding to coarse aggregate and 4 to fine aggregate) was applied.

In the comparison between simulated and experimental data a mismatch was found for lower strain rates. These results pointed out the two important phenomena need to be carefully studied: the stiffening of the binder in thin-films due to the complex behavior of asphalt and the scale dependency of fracture energy.
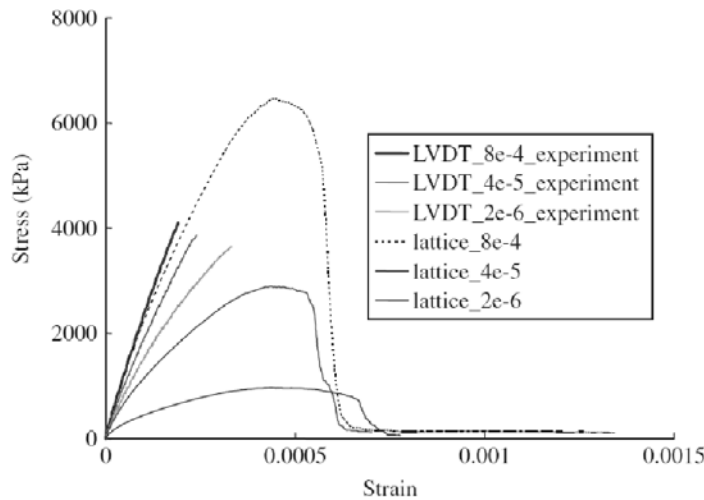
Figure 16: Lattice simulation vs. experimental stress - strain curves (56)

Marasteanu et al. (35, 57) used Acoustic Emission test to estimate the micro-structual phenomenon and the corresponding macroscopic behavior in the asphalt mixtures at low temperature conditions. IDT creep and strength tests were performed and different load levels were applied in the creep configuration to investigate its effect on the development of the micro damage. Three test temperatures, −12°C, −24°C, and −36°C were selected based on the PG lower limit of the asphalt binder.

An AE device with eight-channel recording systems was used to monitor the asphalt mixture specimens during creep and strength tests. The AE events were estimated for the three different temperature conditions showing very few AE events at the beginning of the test until a constant AE rate of 7 to 8 events per second is reached. Overall, before the loading level applied in the creep test was reached, more than 100 AE events were recorded.

For different loading condition and constant temperature, more events were counted during the creep test with higher load level. By using different transducers placed at various locations on the specimen the source location of the AE events was determined on the basis of the differences in time of signals arrival. Since only 143 events were located with 10 mm error for the creep test under the lower loading level at −24°C, this value was selected and a 90% confidence region for AE signals was investigated to evaluate the effect of temperature. The different shape and skewness of the region indicated that, due to its heterogeneity, asphalt mixture properties can be affected by air voids and aggregate distribution. Also the area with micro cracking inside the region (damage zone) showed a shape change with temperature in the case of strength test.

In general it was found that at higher load levels during creep test more events were recorded than at lower load levels for all test temperatures suggesting that micro damage occurs during creep phase.

Marasteanu et.al (58) also applied Acoustic emission (AE) and AE energy to the study of the FPZ (fracture process zone) under a semi circular bending test (SCB) configuration. The stress intensity factor K and the critical stress intensity factor was evaluated according to Lim et al. (59) procedure and the fracture work was evaluated as the area under the loading-deflection

curve. The fracture energy, G_f, was computed by dividing the fracture work by the ligament area (ligament length x specimen thickness) as:

$$G_f = \frac{W_f}{A_{lig}} \qquad \text{and} \qquad W_f = \int pdu \qquad\qquad [17]$$

where:

W_f = fracture work

A_{lig} = area of a ligament

The occurrence of the AE events, the cumulative number, and the rate of occurrence, amplitude distribution, energy and frequency distribution were also evaluated. The AE energy was related to the fracture resistant of the material and to the square of the voltage of the electric signals as:

$$E_i = \int_0^{t_{ae}} V_i^2(t)dt \qquad\qquad [18]$$

where:

E_i = AE energy for channel i

V_i = recorded voltage transient for channel i

t_{ae} = duration of the event for channel i.

The volume affected by micro cracks accumulations was detected as the location in the specimen where more than the 95% of the total AE energy is reached before the peak load. Three specimens were tested for 8 different mixtures with two voids content (4% and 7%) at three different temperatures correlated to the binder performance grade: binder PG -2°C (-30°C), PG + 10°C (-18°C) and PG + 22°C (-6°C). The results showed that temperature has a significant effect on fracture properties: fracture energy increased and fracture toughness decreased as the test temperature increased. Moreover more AE events were detected at low temperature than at high temperature. The ANOVA statistical analysis performed to evaluate the three parameters aggregate, asphalt content and air voids showed that aggregate type is an important factor both for fracture energy and toughness and also that the FPZ is highly affected by air voids level and aggregate type, but is less sensitive to asphalt content (Figure 17).
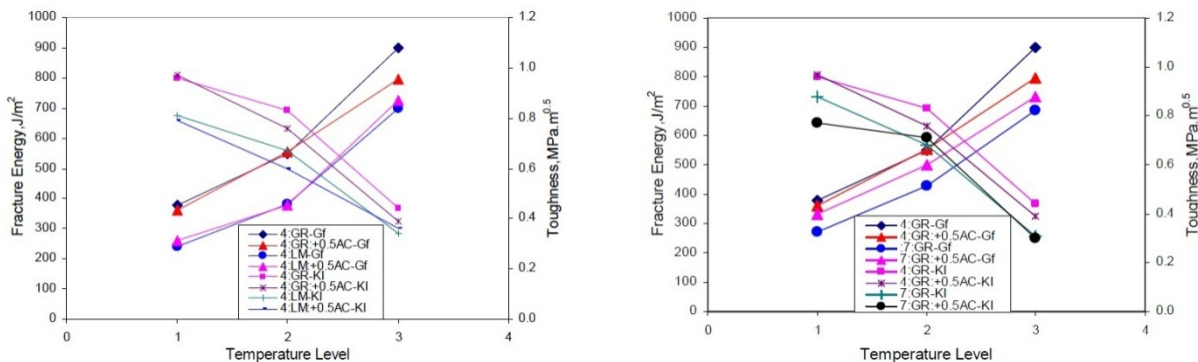
Figure 17: Aggregate and Air voids Comparison (58)

Asphalt Research Consortium

The Asphalt Research Consortium (ARC) (60) is composed by several research groups and it is coordinated by Western Research Institute with partners Texas A&M University, the University of Wisconsin-Madison, the University of Nevada Reno, and Advanced Asphalt Technologies. The research plans were grouped into seven areas, Moisture Damage, Fatigue, Engineered Paving Materials, Vehicle-Pavement Interaction, Validation, Technology Development, and Technology Transfer.

The work element E2d: Thermal Cracking Resistant Mixes for Intermountain States (in the Engineered Paving Materials area) is the part of ARC research project that is related to the topic of the Pooled Fund Study Phase II. The objective of ARC research is to develop a binder/mix evaluation and testing system that could effectively simulate the long term properties of HMA mixtures in the intermountain region and to assess the impact of such properties on the resistance of HMA mixtures to thermal cracking. More specifically the objective of the experimental work element E2d is a system that can simulate the field aging and the thermal cracking process of HMA mixtures. It comprises several sub-tasks:

- E2d-1: Identify Field Sections
- Subtask E2d-2: Identify the Causes of the Thermal Cracking
- Subtask E2d-3: Identify an Evaluation and Testing System
- Subtask E2d-4: Modeling and Validation of the Developed System
- Subtask E2d-5: Develop a Standard

During the first year of activity, the experimental plan was developed and the materials for the various experiments were identified and obtained; moreover, the field sections were selected. The criteria used for the selection of sites included the availability of hourly temperature profiles throughout the depth of the HMA layer, availability of materials properties, and availability of long-term performance data. The relationship between pavement's thermal cracking and the glass transition behavior of asphalt binders and mixtures was considered.

In order to study the glass transition of ten binders, a dilatometric system for measuring binder properties was used. From the results it was noticed that there was a variation in the glass transition behavior as function of the binder grade and modification. Moreover, it was found that binder glass transition properties do not correlate with the glass transition temperature, T_g, of the mixtures. This fact is and indication of the importance of aggregate characteristics and mixture compaction data for mixture thermo-volumetric properties. Furthermore, the contraction and dilation behavior of mixtures showed a hysteretic response.

In order to simulate the temperature gradient and strain distribution in 2.5-in by 2.5-in cross-section mix specimen during thermal cycling, a finite difference model was developed. The heat diffusion equation considered was:

$$\frac{\partial T(x,z,t)}{\partial t} = k \cdot \left(\frac{\partial^2 T(x,z,t)}{\partial x^2} + \frac{\partial^2 T(x,z,t)}{\partial z^2} \right) \qquad [19]$$

Where:

k = thermal diffusivity

T(x,z,t)= specimen temperature as function of space and time

and distribution of the temperature was computed for heating and cooling cycle (Figure18).
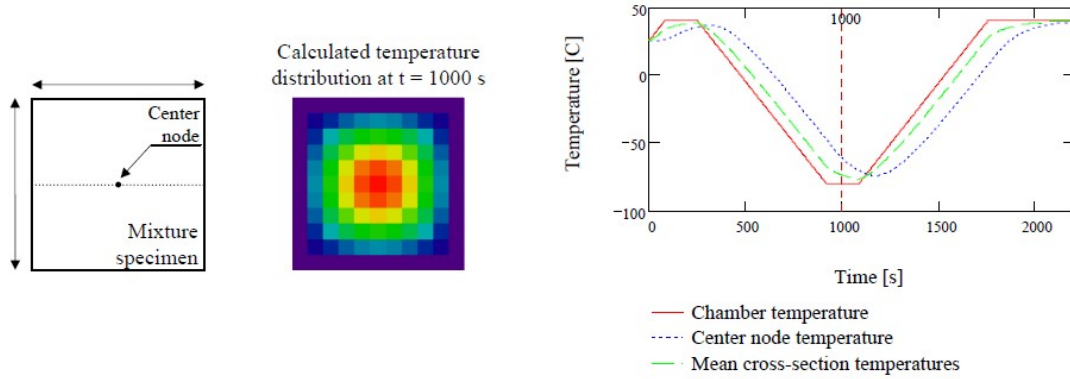
Figure 18: Temperature distribution (60)

It was shown that a single thermocouple could not be reliable to explain the true response of the asphalt mixture. Figure 19 shows the calculated thermal strain of specimen where a looping response was detected.
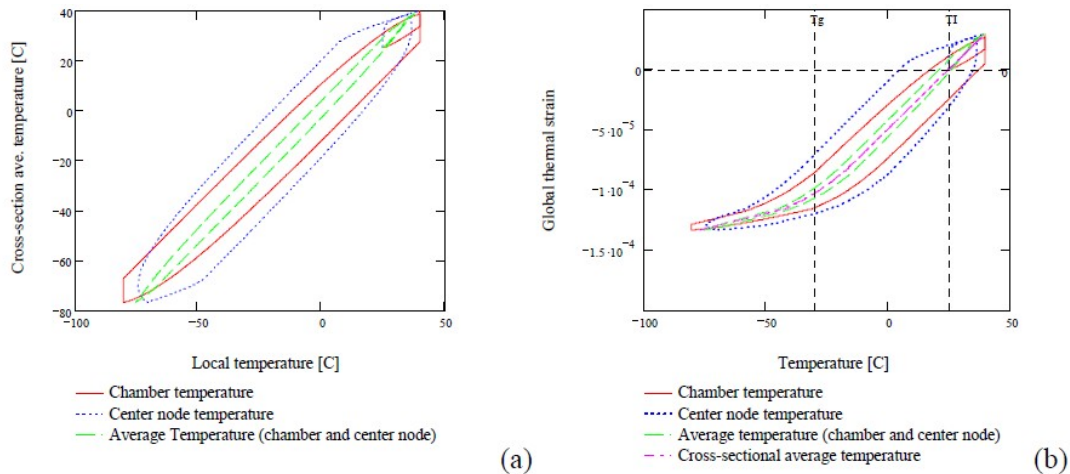
Figure 19: Modeled thermal temperature and strain (60)

The objectives of the second year of investigation include the analysis of the available data on the long-term aging of binders, the evaluation of the impact of aggregate properties on the aging of binders, and the development of an effective testing system for HMA.

MNROAD Reconstruction and Low Temperature Research

Most of the asphalt mixtures and binders used in this study were used in test cells built as part of MnROAD Phase II Construction, which began in 2007. A comprehensive report, documenting the construction effort was recently published (61). Apart from the current study, a few other studies were performed related to the test cells used in the present study or to low temperature behavior.

In one recent study (62), the use of Polyphosphoric acid (PPA) to improve the performance of binders was investigated. A 12.5 mm Superpave mix with 4% air voids and no RAP was used during the investigation. Two sets of cell were dedicated to this research:

27

- Cells 33-35, specifically dedicated to the acid study
- Cells 77-79, dedicated to a fly ash study, that have the wearing course made with PPA+Elvaloy modified binder. For these cells, the base was reclaimed up to 10" to the subgrade plane. Stabilization with fly ash was performed for cell 79. Cell 78 was selected as reference, since the same base used in cells 33-35 was applied. This allowed for a comparison between the acid study and the fly ash study.

Table 1 presents the volumetric data of the mixture used. It may be noticed that a larger amount of air voids is present in the PPA+Elvaloy mixture.

	Test	Cell 33	Cell 34	Cell 35	Cell 77	Cell 79
Loose Mix	Ig Oven AC%	5.4	5.5	5.4	5.2	5.3
	%Fine Agg Angularity	46	46		46	45
	% Coarse Agg Angularity	100/-	100/-	100/-	100/-	100/-
	Gmm	2.478	2.474	2.471	2.484	2.478
	Gmb @ N-design	2.378	2.389	2.379	2.403	2.355
	%Air Voids @ N-design	4.0	3.4	3.7	3.3	5.0
	VMA	16.4	16.2	16.5	15.6	17.2
	VFA	75.4	78.8	77.4	78.8	71.1
Field Cores	% Max Density	94.2	93.5	93.6	92.2	92.1
	% Air Voids	5.8	6.5	6.4	7.8	7.9

Table 1: HMA Field testing data (62)

Field Performance

The field performance of the test sections was evaluated by means of the falling weight deflectometer, rutting measurements, and IRI evaluation. Laboratory tests were also performed both on binders and mixtures. Three testing condition were applied to binder: tank binder, RTFOT (Rolling thin film oven test) aged, and recovered from field cores (field aging). The recovered binder was also subjected to PAV aging showing in two cases a significant increasing in stiffness at low temperature. Field mixtures were used to perform APA ruts tests and Wet Hamburg tests. Dynamic modulus tests at different temperatures and frequencies were run showing a good behavior of PPA+Elvaloy mixture (Figure 20). The investigators concluded that almost no cracking and rutting were observed in the new cells. The laboratory tests, however, indicated that the combination of PPA + polymer will perform better than the PPA alone.
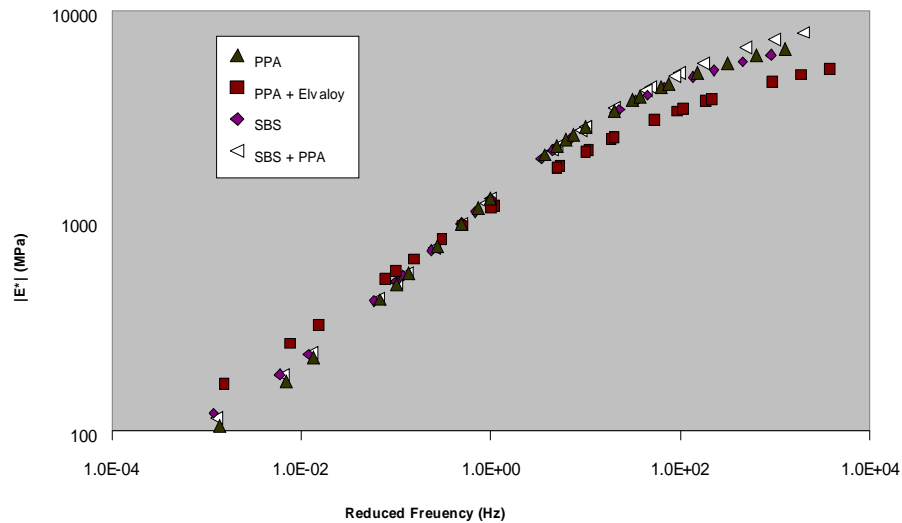
Figure 20: Dynamic Modulus Master Curves (62)

In another study, very recently completed (63), low temperature testing was performed for an additional set of fourteen asphalt mixtures used in the 2008 MnROAD reconstruction project. Limited data analysis was performed in this effort since the focus was on obtaining experimental results.

Conclusion

In the past four years researchers have performed extensive research to better understand the mechanism of low temperature cracking and to develop new test procedures and better pavement models to improve asphalt pavements performance. Some of the most notable findings are:

- More and more researchers are using fracture tests to evaluate low temperature cracking resistance and to model pavement performance
- Physical hardening effects made a come-back and are considered in a new specification in Canada
- Size effects in fracture testing were experimentally evaluated and the effects are being incorporated in pavement prediction models
- New tools, such as acoustic emission, are being used to understand the crack propagation phenomenon.
- Low temperature testing of small beams of asphalt mixture and asphalt sealants has been shown to provide critical information on the low temperature properties of these materials and new specifications are being proposed.

References

(1). American Association of State Highway and Transportation Officials (AASHTO) Standard T 313-08 (2008), "Standard Method of Test for Determining the Flexural Creep Stiffness of Asphalt Binder Using the Bending Beam Rheometer (BBR) ", *Standard Specifications for Transportation Materials and Methods of Sampling and Testing, 29th Edition*, Washington, D.C.

(2). American Association of State Highway and Transportation Officials (AASHTO) Designation T314-07 (2007), "Standard Method of Test for Determining the Fracture Properties of Asphalt Binder in Direct Tension (DT) ", *Standard Specifications for Transportation Materials and Methods of Sampling and Testing* "29nd Edition, Washington, D.C.

(3). American Association of State Highway and Transportation Officials (AASHTO) Designation M320-05 (2002), "Standard Specification for Performance Graded Asphalt Binder", *Standard Specifications for Transportation Materials and Methods of Sampling and Testing* "29nd Edition, Washington, D.C.

(4). American Association of State Highway and Transportation Officials (AASHTO) Standard R28-06, "Standard practice for accelerated aging of asphalt binder using a Pressurized Aging Vessel (PAV)", *Standard Specifications for Transportation Materials and Methods of Sampling and Testing,* 26th Edition, 2006.

(5). American Association of State Highway and Transportation Officials (AASHTO) Designation T322-07 (2009), "Standard Method of Test for Determining the Creep Compliance and Strength of Hot-Mix Asphalt (HMA) Using the Indirect Tensile Test Device", *Standard Specifications for Transportation Materials and Methods of Sampling and Testing,* 29nd Edition, Washington, D.C.

(6). Hallin J., (2004), *Development of the 2002 Guide for the Design of New and Rehabilitated Pavement Structures: Phase II*, National Cooperative Highway Research Program, NCHRP 1-37A, Washington, D.C.

(7). Hase M., Oelkers C., (2009) "Influence of low temperature behaviour of PmB on life cycle", *Proceding of the 7th International RILEM Symposium ATCBM09 on Advanced Testing and Characterization of Bituminous Materials,* 23-32.

(8). Deutsches Institut für Normung DIN EN 14771 (2005): "Bitumen und bitumenhaltige Bindemittel—Bestimmung der Biegesteifigkeit— Biegebalkenrheometer (BBR)" according EN 14771 (2005): "Bitumen and bituminous binders— Determination of the flexural creep stiffness—Bending Beam Rheometer (BBR)".

(9). Khedoe R., Molenaar A., & v.d. Ven M., (2008), "Low temperature behavior of very hard bituminous binder material for road applications" *Proceeding of the 6th RILEM conference on Cracking in Pavement,* 481-490.

(10). Yee P., Aida N., Hesp S.A.M., Marks P. and Tam K. K., (2006), "Analysis of Premature Low-Temperature Cracking in Three Ontario, Canada, Pavements", *Transportation Research Record*, 1962, 44–51.

(11). Struik L. C. E., (1978), *Physical Ageing in Amorphous Polymers and Other Materials.* Elsevier Scientific Publishing Co., Amsterdam, Netherlands.

(12). Bahia, H.U. Low-Temperature Isothermal Physical Hardening of Asphalt Cements. Ph.D. Thesis, Pennsylvania State University, December 1991.

(13). Al-Qadi I. L., HseinYang S., Dessouky S. and Masson J. F., (2007), "Development of Crack Sealant Bending Beam Rheometer (CSBBR) Testing to Characterize Hot-Poured Bituminous Crack Sealant at Low Temperature", *Journal of the Association of Asphalt Paving Technologists*, Vol. 76, 85-122

(14). Zanzotto L., (1996), *Laboratory Testing of Crack Sealing Materials for Flexible Pavements*, Final Report, Transportation Association of Canada, Ottawa, ON, 171 pp.

(15). Zofka A., Marasteanu M, Li X., Clyne T., Jim McGraw J., (2005), "Simple Method to Obtain Asphalt Binders Low Temperature Properties from Asphalt Mixtures Properties", *Journal of the Association of Asphalt Paving Technologists*, Vol. 74, 255-282.

(16). Elseifi M., Dessouky S., Al-Qadi I. L. and Yang S-H., (2006), "Viscoelastic Model to Describe the Mechanical Response of Bituminous Sealants at Low Temperature", *Transportation Research Record,* 1958, 82-89.

(17). Velásquez R., Marasteanu M., Turos M., Labuz J., (2009), "Effect of beam size on the creep stiffness of asphalt mixtures at low temperatures", *Proceding of the 7th International RILEM Symposium ATCBM09 on Advanced Testing and Characterization of Bituminous Materials*, 313-322.

(18). Apeagyei A. K., Buttlar W. G. and Dempsey B. J., (2008), "Investigation of Cracking Behavior of Antioxidant-Modified Asphalt Mixtures", *Journal of the Association of Asphalt Paving Technologists*, Vol. 77, 519-545

(19). Kim Y. R., King Y. and Momen M., (2004), "Dynamic Modulus Testing of Asphalt Concrete in Indirect Tension Mode", *Transportation Research Record*, 1891, 163–173.

(20). Katicha S., Flintsch G., (2009), "Theoretical investigation of the stress distribution in a Bimodular IDT specimen", *Proceding of the 7th International RILEM Symposium ATCBM09 on Advanced Testing and Characterization of Bituminous Materials*, 453-462.

(21). Ambartsumyan S., (1965), "The axisymmetric problem of circular cylindrical shell made of materials with different stiffness in tension and compression", *Izv. Akad. Nauk. SSR Mekh.* 4, 77–85.

(22). Ambartsumyan S., and Khachartryan A., (1969), "Basic equations and relations of the different modulus theory of elasticity of an anisotropic body", *Mechanics of Solids*, 4, 48-56.

(23). Birgisson B., Montepara A., Romeo E., Roque1 R. and Tebaldi G., (2007), "The displacement discontinuity method for predicting HMA fracture energy in the bending beam test", *Proceeding of the International Conference on Advanced Characterization of Pavement and Soil Engineering Materials*, 69-77.

(24). Sauzéat C., Di Benedetto H., Chaverot P. and Gauthier G., (2007), "Low temperature behavior of bituminous mixes: TSRS tests and acoustic emission", *Proceeding of the International Conference on Advanced Characterisation of Pavement and Soil Engineering Materials*, 1263-1272.

(25). Hase M., Oelkers C., (2009), "Influence of low temperature behaviour of PmB on life cycle", *Proceding of the 7th International RILEM Symposium ATCBM09 on Advanced Testing and Characterization of Bituminous Materials*, 23-32.

(26). Janoo V., (1989), Performances *of 'Soft' Asphalt Pavements in Cold Regions* USA CRREL Special Report.

(27). Koh C., Lopp G. and Roque R., (2009), "Development of a Dog-Bone Direct Tension Test (DBDT) for asphalt concrete", *Proceding of the 7ᵗʰ International RILEM Symposium ATCBM09 on Advanced Testing and Characterization of Bituminous Materials,* 585-596.

(28). ASTM Method E399-90, "Plane-Strain Fracture Toughness for Metallic Materials", *Annual book of ASTM Standards, Vol. 03.01.* (2002) American Society for Testing and Materials, Philadelphia, PA

(29). Portillo O. and Cebon D., (2008), "An experimental investigation of the fracture mechanics of bitumen and asphalt", *Proceeding of the 6ᵗʰ RILEM conference on Cracking in Pavement*, 627-636.

(30). Harvey J.A.F. & Cebon D., (2003), "Failure Mechanism in Viscoelastic Films", *Journal of Materials Science*, 38, 1021–1032.

(31). Genin G.M. and Cebon D., (2000), "Fracture Mechanics in Asphalt Concrete", *Road Materials and Pavement Design*, 1(4): 419–450.

(32). Harvey J. A. F. and Cebon D., (2005), "Fracture Tests on Bitumen Films", *Journal of Material in Civil Engineering*, Vol. 17, Issue 1, 99-106.

(33). Wagoner M.P. and Buttlar W.G., (2007), "Influence of specimen size in fracture energy of asphalt concrete", *Journal of the Association of Asphalt Paving Technologists*, Vol. 76, 391-426

(34). Bazant Z.P. (1984), "Size effect in blunt fracture: concrete, rock, metal", *Journal of Engineering Mechanics*, Vol.110, No 4, 518-535.

(35). Marasteanu M., Li X., Labuz J., (2006), "Observation of Crack Propagation in Asphalt Mixtures Using Acoustic Emission", *presented at Transportation Research Board 85ᵗʰ Annual Meeting*.

(36). Kim H., Partl M. N., Wagoner M.P., Buttlar W. G., (2009), "Size effect investigation on fracturing of asphalt concrete using the cohesive softening Discrete Element Model", *Proceding of the 7ᵗʰ International RILEM Symposium ATCBM09 on Advanced Testing and Characterization of Bituminous Materials*, 827-836.

(37). Kim H., Wagoner M. P. and Buttlar W. G., (2007), "Fracture modeling considered rate – dependency of asphalt concrete using discrete element method", *Proceeding of the International Conference on Advanced Characterization of Pavement and Soil Engineering Materials*, 79-92.

(38). Hu X., Wittmann F., (2002), "Size Effect on Toughness Induced by Crack Close to Free Surface", *Engineering Fracture Mechanics*, Vol. 69,555-562.

(39). Chong K. and Kuruppu M., (1984), "New Specimen for Fracture Toughness Determination for Rock and Other Materials", *International Journal of Fracture*, Vol. 26, R59-R62.

(40). Van Rooijen R. C. and de Bondt A. H., (2008), "Crack propagation performance evaluation of asphaltic mixtures using a new procedure based on cyclic Semi-Circular Bending test (SCB)", *Proceeding of the 6ᵗʰ RILEM conference on Cracking in Pavement*, 437-446.

(41). European Committee for Standardization (CEN), EN 13589, CEN/TC 336 - Bituminous binders, EN 13589:2008, Bitumen and bituminous binders - Determination of the tensile properties of modified bitumen by the force ductility method.

(42). European Committee for Standardization (CEN), EN 13589, CEN/TC 336 - Bituminous binders, EN 13703:2003, Bitumen and bituminous binders - Determination of deformation energy.

(43). Perez F., Botella R., Valdes G., (2009), "Experimental study on resistance to cracking of bituminous mixtures using the Fenix test", *Proceeding of the 7ᵗʰ International RILEM*

Symposium ATCBM09 on Advanced Testing and Characterization of Bituminous Materials, 707-714.

(44). Zbrowski A. and Kaloush K. E., (2007), "Predictive equation to Evaluate Thermal Fracture of Asphalt Rubber Mixtures", *Road materials and pavement design*, Vol. 8, n°4, pp. 819-833.

(45). Kim J., Roque R. and Birgisson B., (2008), "Integration of thermal fracture in the HMA fracture *model", Journal of the Association of Asphalt Paving Technologist*, Vol. 77, 631-661.

(46). Roque R., Birgisson B., Zhang Z., Sangpetngam B., and Grant T., (2002), *Implementation of SHRP Indirect Tension Tester to Mitigate Cracking in Asphalt Pavements and Overlays*, Final Report, FDOT BA-546, University of Florida, Gainesville, FL.

(47). Roque R., Birgisson B., DrakosC , and Dietrich B., (2004), "Development and Field Evaluation of Energy-Based Criteria for Topdown Cracking Performance of Hot Mix Asphalt," *Journal of the Association of Asphalt Paving Technologists*, Vol. 73, pp. 229-260.

(48). Zhang Z., Roque R., Birgisson B. and Sangpetngam B., (2001), "Identification and Verification of a Suitable Crack Growth Law", *Journal of the Association of Asphalt Paving Technologists*, Vol. 70, 206-241.

(49). Apeagyei A. K., Dave E. V. and Buttlar W. G., (2008), "Effect of cooling rate on thermal cracking of asphalt", *Journal of the Association of Asphalt Paving Technologist*, Vol. 77, 709-738.

(50). Marasteanu M., Zofka A., Turos M., Li X., Velasquez R, Buttlar W., Paulino G., Braham A., Dave E., Ojo J, Bahia H., Williams C., Bausano J., Kvasnak A., Gallistel A., McGraw J., (2007), *Investigation of Low Temperature Cracking in Asphalt Pavements National Pooled Fund Study 776*, Final Report prepared for Minnesota Department of Transportation Research Services MS 330, University of Minnesota, Minneapolis, MN.

(51). Dave E. V., Braham A. F., Buttlar W. G., Paulino G. H. and Zofka A., (2008), "Integration of laboratory testing, field performance data and numerical simulations for the study of low-temperature cracking", *Proceeding of the 6th RILEM conference on Cracking in Pavement*, 369-378.

(52). Wistuba M, and Spiegl M., (2007), " Asphalt Pavement in Cold Climates – A Systematic Approach for the Assessment of Cracking Resistance", *Proceeding of the International Conference on Advanced Characterization of Pavement and Soil Engineering Materials*, 1199-1208.

(53). Bae A., Stoffels S., Chehab G, Clyne T. and Worel B., (2007) , "Direct effects of thermal cracks on pavement roughness", *Journal of the Association of Asphalt Paving Technologists*, Vol. 76, 59-84.

(54). Cundall, P. A. and Strack, O. D. L., (1979), "A discrete numerical model for granular assemblies", *Géotechnique,* 29, 47–65.

(55). Wu J., A. Collop A. and McDowell G., (2008), " Discrete element modeling of low temperature monotonic compression tests in an idealized asphalt mixture", *Proceeding of the 6th RILEM conference on Cracking in Pavement*, 395-403.

(56). Feng Z, Zhang P., Guddati M. N., Kim Y. R. and Little D. N., (2008), " Virtual testing procedure for cracking performance prediction of HMA", *Proceeding of the 6th RILEM conference on Cracking in Pavement*, 575-585.

(57). Marasteanu M., Labuz J. and Li X., (2008), "Acoustic emission in asphalt mixture IDT creep and strength tests", *Proceding of the $7th$ International RILEM Symposium ATCBM09 on Advanced Testing and Characterization of Bituminous Materials*, 501-508.

(58). Marasteanu M., Li X. and Turos M., (2007), "Study of low temperature cracking in asphalt mixtures using mechanical testing and acoustic emission", *Journal of the Association of Asphalt Paving Technologists*, Vol. 76, 427-453.

(59). Lim I. L., Johnston I. W., and Choi S. K., (1993), "Stress Intensity Factor for Semi Circular Specimen under Three-Point Bending", *Engineering Fracture Mechanics*, Vol. 44, No.3, 363-382.

(60). Asphalt Research Consortium, *Annual Work Plan for Year 2 – Revised*, April 1, 2008 – March 31, 2009 December 2008 (Western Research Institute, Texas A&M University, University of Wisconsin-Madison, University of Nevada-Reno, Advanced Asphalt Technologies)

(61). Johnson, A., Clyne, T. R., Worel, B. J., "2008 MnROAD Phase II Construction Report," Minnesota Department of Transportation, June 2009.

(62). Clyne T. R., Johnson E. N., James McGraw J. and Reinke G., (2009), *Field Investigation of Polyphosphoric Acid Modified Binders at MnROAD*, Minnesota Department of Transportation Office of Materials.

(63). Marasteanu M., Moon, K. H., Turos M. I., "Asphalt Mixture and Binder Fracture Testing for 2008 MnROAD Construction," Minnesota Department of Transportation, December 2009.